SCIPEDIA

Matrix Algorithms Based on Jacobi and Romanovski-Jacobi Polynomials for Solving the FitzHugh-Nagumo Nonlinear Equation

Ramy Hafez[1], Salah Boulaaras[2,*] and Hamiden Abd El-Wahed Khalifa[2]

[1] Department of Mathematics, Faculty of Education, Matrouh University, Marsa Matrouh, 51511, Egypt

[2] Department of Mathematics, College of Science, Qassim University, Buraydah, 51452, Saudi Arabia

INFORMATION

Keywords:
Jacobi polynomials
collocation points
Romanovski-Jacobi functions
FitzHugh-Nagumo nonlinear equation
operational matrix equations
numerical methods
efficiency

DOI: 10.23967/j.rimni.2025.10.63315

SCIPEDIA Revista Internacional de Métodos Numéricos para Cálculo y Diseño en Ingeniería

RIMNI Revista Internacional Métodos numéricos para cálculo y diseño en ingeniería

Matrix Algorithms Based on Jacobi and Romanovski-Jacobi Polynomials for Solving the FitzHugh-Nagumo Nonlinear Equation

Ramy Hafez[1], **Salah Boulaaras**[2,*] **and Hamiden Abd El-Wahed Khalifa**[2]

[1]Department of Mathematics, Faculty of Education, Matrouh University, Marsa Matrouh, 51511, Egypt

[2]Department of Mathematics, College of Science, Qassim University, Buraydah, 51452, Saudi Arabia

ABSTRACT

The present paper develops and makes efficient, a new, state-of-the-art numerical technique for solving the FitzHugh-Nagumo Nonlinear Equation (FH-NNE) with initial and boundary conditions, which represents perhaps the simplest mathematical model for discussing biological systems, including nerve signals and cardiac behavior. Which consists of operational matrices and spectral techniques based on Jacobi and Romanovski-Jacobi polynomials. It is ensured that the nonlinear system is modeled so accurately that it can be effectively solved to ensure the best accuracy combined with computational economy. Comparing the results with the respective numerical results, it is seen that the proposed techniques outdo the standard ones as respects accuracy and efficiency of computation.

OPEN ACCESS

Received: 11/01/2025

Accepted: 25/02/2025

Published: 07/04/2025

DOI
10.23967/j.rimni.2025.10.63315

Keywords:
Jacobi polynomials
collocation points
Romanovski-Jacobi functions
FitzHugh-Nagumo nonlinear equation
operational matrix equations
numerical methods
efficiency

1 Introduction

The FitzHugh-Nagumo equation is a well-known mathematical model that describes key biological processes, such as the transmission of nerve impulses through the nervous system and electrical activity in cardiac tissues. The nonlinear structure makes accurate numerical solutions by classical methods very difficult to obtain [1–5]. This, therefore, generates an urgent need to work on advanced and efficient numerical techniques for the solution of these equations [6–9]. This study introduces a novel numerical framework based on Jacobi and Romanovski-Jacobi polynomials for solving the FitzHugh-Nagumo equation. The proposed methodology combines spectral methods with operational matrices, offering a highly efficient and precise approach for tackling complex mathematical

*Correspondence: Salah Boulaaras (s.boularas@qu.edu.sa).

problems [10–12]. The primary objective is to develop numerical solutions that outperform traditional finite-difference and finite-element methods in terms of accuracy and computational efficiency [13–16]. Jacobi and Romanovski-Jacobi polynomials are chosen for their excellent convergence properties and their suitability for representing nonlinear dynamic systems. These polynomials have been shown to minimize computation errors and optimize the performance of numerical methods [17–19]. In this study, the operational matrices from these polynomials utilize collocation points, forming a new spectral method [20,21]. This newly developed approach is an important step forward in numerical algorithms for solving nonlinear equations by taking advantage of advanced mathematical tools [22]. The proposed method has several legit implications in fields like cardiac modeling, neuroscience, and other physical systems where nonlinear dynamics are significant [23,24]. It leads to significantly greater accuracy in solutions and shorter computation times compared to existing methods [25–27]. The key objectives of this study are as follows:

- For the preparation of a new numerical framework for the FitzHugh-Nagumo equation based on Jacobi and Romanovski-Jacobi polynomials.
- To evaluate the competency of the suggested procedure concerning both accuracy and computational efficiency in comparison with conventional numerical techniques.
- To study how different parameters influence the accuracy of numerical solutions.

This underscores the necessity of developing efficient numerical methods for nonlinear Partial differential equations (PDEs), which include the FitzHugh-Nagumo equation, in order to obtain a better understanding of the intricate biological and physical systems [28,29]. Standard numerical methods frequently suffer tasks from inefficiency in computations and accuracy demands engendered, by such stiff systems and long-term simulations [30–32]. The proposed methods advance forward, by using several distinct features of Jacobi and Romanovski-Jacobi polynomials, the use of which is thought to give rise to much better-suited approximations and an overall faster convergence in comparison to classical basis functions [33–35]. Therefore, immense relief extends one step further since the method becomes both quicker and explicable in rendering large-scale application [36,37]. Coupled with that is the flexibility of the proposed framework for seamless switching applications from one nonlinear PDE to the other, thus allowing for wider reach across varying fronts of research fields [38,39]. The present work gives builds a powerful tool for the researcher and practitioners working with complex dynamical systems through its fusion of spectral methods and operational matrices [40,41]. The results of this research project will be utilized in areas such as computational biology, computational neuroscience, and engineering, where numerical simulations have to strike a perfect balance between accuracy and computational efficiency [42–44].

This algorithm has indeed been utilized to achieve the solution of the FitzHugh-Nagumo nonlinear equation (FH-NNE). The key contributions and aspects of the research conducted are summarized as follows:

i) A new numerical method is introduced that incorporates Jacobi and Romanovski-Jacobi polynomials to effectively cope with the nonlinearities and stiffness of the FH-NNE.
ii) Derivative-specific operational matrices are constructed using these polynomials, which significantly reduce the effort in approximating derivatives in the spectral domain.
iii) The proposed method exhibits greater accuracy and computational speed compared to the conventional numerical methods.
iv) The spectral collocation method exploits the orthogonal characteristics of these polynomials, rendering it particularly apt for domains including rapid variations or steep gradients.

v) The model is formulated with generalizability in mind so that it can be used for other nonlinear partial differential equations apart from the FH-NNE.

vi) All these put together constitute a major development in numerical methods of solving complicated nonlinear systems.

The organization of the paper is as follows: Section 2 reviews that of shifted Jacobi and Romanovski-Jacobi polynomials, including operational matrices of derivatives, which are the basis for the proposed algorithms. Section 3 details a matrix method to solve the FitzHugh-Nagumo nonlinear equation. Section 4 presents examples demonstrating the efficacy of the method. In Section 5, concluding remarks are given, along with observations regarding the findings and future avenues of research.

2 A Brief Introduction to Jacobi and Romanovski-Jacobi Polynomials

This section focuses on describing the basis functions utilized in our proposed spectral algorithm. To begin, we provide an overview of key concepts related to the Jacobi and Romanovski-Jacobi (RJ) polynomials.

2.1 The Main Feature of Jacobi Basis Functions

The Jacobi polynomials (JPs) are fundamental in various areas of mathematics [1]. They are orthogonal and correspond to the weight function $\varpi(\varkappa) = (1-\varkappa)^{\alpha}(1+\varkappa)^{\beta}$ over the interval $[-1,1]$, with $\alpha,\ \beta > -1$. We denote the $\hat{r}-$th degree Jacobi polynomial of order $\alpha,\ \beta$ by $J_{\hat{r}}^{\alpha,\beta}(\varkappa)$. One of its explicit forms for this class of polynomials is presented below:

$$(1-\varkappa)^{\alpha}(1+\varkappa)^{\beta}J_{\hat{r}}^{\alpha,\beta}(\varkappa) = \frac{(-1)^{\hat{r}}}{2^{\hat{r}}\hat{r}!}\frac{d^{\hat{r}}}{d\varkappa^{\hat{r}}}\left[(1-\varkappa)^{\hat{r}+\alpha}(1+\varkappa)^{\hat{r}+\beta}\right]. \tag{1}$$

This formula is referred to as the Rodrigues formula for $\hat{r} = 0, 1, 2, \ldots$

The shifted Jacobi polynomials (SJPs) are defined on the interval $[0, \mathcal{L}]$, where $\mathcal{L} > 0$, using the variable transformation $\varkappa \to -1 + \dfrac{2\varkappa}{\mathcal{L}}$. This transformation leads to the SJPs, denoted by $\mathcal{J}_{\hat{r}}^{\alpha,\beta}(\varkappa) = J_{\hat{r}}^{\alpha,\beta}\left(-1+\dfrac{2\varkappa}{\mathcal{L}}\right)$.

The SJPs of degree $\hat{r}$ can be explicitly expressed as follows:

$$\mathcal{J}_{\hat{r}}^{\alpha,\beta}(\varkappa) := \sum_{r=0}^{\hat{r}} \frac{(-1)^{\hat{r}-r}\,\Gamma(\hat{r}+r+\alpha+1)\,\Gamma(\hat{r}+\beta+1)}{\Gamma(\hat{r}+\alpha+\beta+1)\,\Gamma(r+\beta+1)\,(\hat{r}-r)!\;r!\;\mathcal{L}^{r}}\,\varkappa^{r}, \quad \hat{r} \geq 0. \tag{2}$$

The SJPs are also shown to be orthogonal concerning the weight function $\mathfrak{w}_{\mathcal{L}}(\varkappa) = (\mathcal{L}-\varkappa)^{\alpha}\varkappa^{\beta}$. As a consequence, we have

$$\int_0^{\mathcal{L}} \mathcal{J}_{\hat{r}}^{\alpha,\beta}(\varkappa)\,\mathcal{J}_{\hat{s}}^{\alpha,\beta}(\varkappa)\,\mathfrak{w}_{\mathcal{L}}(\varkappa)\,d\varkappa = \begin{cases} \hbar_{\hat{r}}, & \hat{r} = \hat{s}, \\ 0, & otherwise, \end{cases} \tag{3}$$

where $\hbar_{\hat{r}} = \dfrac{\Gamma(\hat{r}+\alpha+1)\Gamma(\hat{r}+\beta+1)\mathcal{L}^{\alpha+\beta+1}}{(2\hat{r}+\alpha+\beta+1)\hat{r}!\,\Gamma(\hat{r}+\alpha+\beta+1)}$. Assume $\vartheta(\varkappa)$ is a polynomial of degree N. It can then be represented using shifted Jacobi polynomials

$$\vartheta(\varkappa) = \sum_{\hat{r}=0}^{N} u_{\hat{r}} \mathcal{J}_{\hat{r}}^{\alpha,\beta}(\varkappa) = \mathbf{U}^T \boldsymbol{\phi}(\varkappa), \tag{4}$$

where the coefficients $u_{\hat{r}}$ are determined by

$$u_{\hat{r}} = \frac{1}{\hbar_{\hat{r}}} \int_0^{\mathcal{L}} \varpi_{\mathcal{L}}(\varkappa)\vartheta(\varkappa)\,\mathcal{J}_{\hat{r}}^{\alpha,\beta}(\varkappa)\,d\varkappa, \qquad \hat{r} = 0, 1, \ldots \tag{5}$$

If the vector of shifted Jacobi coefficients U and the shifted Jacobi vector $\boldsymbol{\phi}(\varkappa)$ are written as

$$\mathbf{U}^T = [u_0, u_1, \ldots, u_N], \tag{6}$$

and

$$\boldsymbol{\phi}(\varkappa) = [\mathcal{J}_0^{\alpha,\beta}(\varkappa), \mathcal{J}_1^{\alpha,\beta}(\varkappa), \ldots, \mathcal{J}_N^{\alpha,\beta}(\varkappa)]^T, \tag{7}$$

respectively, then the first-order derivative of the vector $\boldsymbol{\phi}(\varkappa)$ can be written as

$$\frac{d\boldsymbol{\phi}(\varkappa)}{d\varkappa} = \Delta^{(1)}\boldsymbol{\phi}(\varkappa), \tag{8}$$

where $\Delta^{(1)}$ is the $(N+1)\times(N+1)$ derivative's operational matrix is expressed as

$$\Delta^{(1)} = (d_{\hat{r}\hat{s}}) = \begin{cases} \xi(\hat{r},\hat{s}), & \hat{r} > \hat{s}, \\ 0, & otherwise, \end{cases} \tag{9}$$

where

$$\xi(\hat{r},\hat{s}) = \frac{(\hat{r}+\alpha+\beta+1)(\hat{r}+\alpha+\beta+2)_{\hat{s}}(\hat{s}+\alpha+2)_{\hat{r}-\hat{s}-1}\Gamma(\hat{s}+\alpha+\beta+1)}{\mathcal{L}(\hat{r}-\hat{s}-1)!\,\Gamma(2\hat{s}+\alpha+\beta+1)} \times {}_3F_2\left(\begin{matrix} -\hat{r}+\hat{s}+1, & \hat{r}+\hat{s}+\alpha+\beta+2, & \hat{s}+\alpha+1 \\ \hat{s}+\alpha+2, & 2\hat{s}+\alpha+\beta+2 & \end{matrix}; 1\right), \tag{10}$$

where $(a)_i = \dfrac{\Gamma(a+i)}{\Gamma(a)}$ is the Pochhammer symbol, and for the general definition of a generalized hypergeometric series and the special ${}_3F_2$, see [9]. In general, the hypergeometric series ${}_3F_2$ cannot be summed in explicit form, but it can be summed by Watson's identity [45], if $\alpha = \beta$.

For example, the matrix $\Delta^{(1)}$ for $N = 5$ and $\alpha = \beta = 0$ has the following form:

$$\mathcal{W} = \frac{1}{\mathcal{L}} \begin{pmatrix} 0 & 0 & 0 & 0 & 0 & 0 \\ 2 & 0 & 0 & 0 & 0 & 0 \\ 0 & 6 & 0 & 0 & 0 & 0 \\ 2 & 0 & 10 & 0 & 0 & 0 \\ 0 & 6 & 0 & 14 & 0 & 0 \\ 2 & 0 & 10 & 0 & 18 & 0 \end{pmatrix}_{6\times 6}. \tag{11}$$

Remark 1. *The n-th derivative of the SJPs can be expressed as*

$$\frac{d^n \boldsymbol{\phi}(\varkappa)}{d\varkappa^n} = (\Delta^{(1)})^n \boldsymbol{\phi}(\varkappa), \tag{12}$$

where $n \in \mathbb{N}$. *In addition, the superscript in* $\Delta^{(1)}$ *represents matrix powers. Thus*

$$\Delta^{(n)} = (\Delta^{(1)})^n, \quad n = 1, 2, \ldots \tag{13}$$

2.2 The Essential Part of the Romanovski-Jacobi Basis Functions

The Romanovski-Jacobi (RJ) polynomials represent a unique set of finite orthogonal bases. This class was first presented in [8] and subsequently attracted the interest of researchers for its application in approximating solutions to differential equations [5,6,46]. They are denoted by $\mathcal{R}_{\hat{t}}^{\upsilon,\varepsilon}(\varsigma)$, which is clearly reformulated as

$$\mathcal{R}_{\hat{t}}^{\upsilon,\varepsilon}(\varsigma) := \sum_{t=0}^{\hat{t}} (-1)^t \frac{\Gamma(-\upsilon-\varepsilon-\hat{t})\Gamma(\upsilon+\hat{t}+1)}{t!\,\Gamma(-\upsilon-\varepsilon-\hat{t}-t)\Gamma(\upsilon+t+1)\Gamma(\hat{t}-t+1)} \varsigma^t. \tag{14}$$

The following key property of these Romanovski-Jacobi polynomials (RJPs) is their orthogonality concerning the weight function $\mathfrak{w}_{\mathcal{R}}(\varsigma) \equiv \varsigma^{\upsilon}(1+\varsigma)^{\varepsilon}$. This requires the conditions $\upsilon > -1$ and $\varepsilon < -2M-\upsilon-1$, where $M > 0$ is a specified integer. The orthogonality is defined over the semi-infinite interval $(0, \infty)$. Specifically, we have

$$\int_0^{\infty} \mathcal{R}_{\hat{t}}^{\upsilon,\varepsilon}(\varsigma)\, \mathcal{R}_{\hat{s}}^{\upsilon,\varepsilon}(\varsigma) \mathfrak{w}_{\mathcal{R}}(\varsigma)\, d\varsigma = \begin{cases} \hat{\hbar}_{\hat{t}}, & \hat{t} = \hat{s}, \\ 0, & otherwise, \end{cases} \tag{15}$$

where $\hat{\hbar}_{\hat{t}} = -\dfrac{\Gamma(\upsilon+\hat{t}+1)\Gamma(-\varepsilon-\upsilon-\hat{t})}{(2\hat{t}+\upsilon+\varepsilon+1)\hat{t}!\,\Gamma(-\varepsilon-\hat{t})}$. Assume $\tilde{\vartheta}(\varsigma)$ is a polynomial of degree M. It can then be represented using Romanovski-Jacobi polynomials

$$\tilde{\vartheta}(\varsigma) = \sum_{\hat{\imath}=0}^{M} \hat{u}_{\hat{\imath}} \mathcal{R}_{\hat{\imath}}^{\upsilon,\varepsilon}(\varsigma) = \hat{\mathbf{U}}^T \boldsymbol{\psi}(\varsigma), \tag{16}$$

where the coefficients $\hat{u}_{\hat{\imath}}$ are determined by

$$\hat{u}_{\hat{\imath}} = \frac{1}{\hat{\hbar}_{\hat{\imath}}} \int_0^{\infty} \mathfrak{w}_{\mathcal{R}}(\varsigma) \tilde{\vartheta}(\varsigma)\, \mathcal{R}_{\hat{\imath}}^{\upsilon,\varepsilon}(\varsigma)\, d\varsigma, \qquad \hat{t} = 0, 1, \ldots \tag{17}$$

If the vector of Romanovski-Jacobi coefficients $\hat{\mathbf{U}}$ and the Romanovski-Jacobi vector $\boldsymbol{\psi}(\varsigma)$ are written as

$$\hat{\mathbf{U}}^T = [\hat{u}_0, \hat{u}_1, \ldots, \hat{u}_M], \tag{18}$$

and

$$\boldsymbol{\psi}(\varsigma) = [\mathcal{R}_0^{\upsilon,\varepsilon}(\varsigma), \mathcal{R}_1^{\upsilon,\varepsilon}(\varsigma), \ldots, \mathcal{R}_M^{\upsilon,\varepsilon}(\varsigma)]^T, \tag{19}$$

respectively, then the first-order derivative of the vector $\boldsymbol{\psi}(\varsigma)$ can be written as

$$\frac{d\boldsymbol{\psi}(\varsigma)}{d\varsigma} = \Theta^{(1)} \boldsymbol{\psi}(\varsigma), \tag{20}$$

where $\Theta^{(1)}$ is the $(M+1)\times(M+1)$ derivative's operational matrix is expressed as

$$\Theta^{(1)} = (\hat{d}_{\hat{i}\hat{s}}) = \begin{cases} \hat{\xi}(\hat{t},\hat{s}), & \hat{t} > \hat{s}, \\ 0, & otherwise, \end{cases} \tag{21}$$

where

$$\hat{\xi}(\hat{t},\hat{s}) = \frac{-\Gamma(-\hat{s}-\upsilon-\varepsilon)(2\hat{t}+\upsilon+\varepsilon+1)\Gamma(\hat{s}+\upsilon+1)\Gamma(-\hat{s}-\upsilon-\varepsilon-1)}{\Gamma(-\hat{s}-\upsilon-\varepsilon-1)\Gamma(-\upsilon-\varepsilon-\hat{t})\Gamma(1+\upsilon+\hat{t})}$$
$$\times \sum_{l=0}^{\hat{s}-\hat{t}-1} \frac{(-1)^{l+1}\Gamma(1-\upsilon-\varepsilon+2\hat{t}-l)\Gamma(1+\upsilon+\hat{t}+l)}{l!\,\Gamma(1-\hat{t}-l+\hat{s}-1)\Gamma(1+\hat{t}+l+\upsilon+1)\Gamma(-\hat{t}-l-\hat{s}-\upsilon-\varepsilon-1)}. \tag{22}$$

For the proof, see [46]. For example, the matrix $\Theta^{(1)}$ for $\upsilon = 2$, $\varepsilon = -40$ and $M = 5$ has the following form:

$$\mathcal{Q} = \begin{pmatrix} 0 & 0 & 0 & 0 & 0 & 0 \\ -36 & 0 & 0 & 0 & 0 & 0 \\ -\frac{245}{6} & -\frac{595}{18} & 0 & 0 & 0 & 0 \\ -\frac{3043}{70} & -\frac{77}{2} & -\frac{1056}{35} & 0 & 0 & 0 \\ -\frac{3916}{85} & -\frac{2104}{51} & -\frac{3069}{85} & -\frac{465}{17} & 0 & 0 \\ -\frac{27416}{561} & -\frac{4340}{99} & -39 & -\frac{6293}{187} & -\frac{812}{33} & 0 \end{pmatrix}_{6\times 6}. \tag{23}$$

Remark 2. *The n-th derivative of the RJPs can be expressed as*

$$\frac{d^n \boldsymbol{\psi}(\varsigma)}{d\varsigma^n} = (\Theta^{(1)})^n \boldsymbol{\psi}(\varsigma), \tag{24}$$

where $n \in \mathbb{N}$. In addition, the superscript in $\Theta^{(1)}$ represents matrix powers. Thus

$$\Theta^{(n)} = (\Theta^{(1)})^n, \quad n = 1, 2, \ldots \tag{25}$$

2.3 A Comprehensive Error Analysis of the Product of Jacobi and Romanovski-Jacobi Basis Functions

We proceed by setting

$$\mathfrak{K} = \Big\{(\varkappa,\varsigma) : \varkappa \in [0,\mathcal{L}],\ \varsigma \in [0,\mathcal{T}]\Big\}, \tag{26}$$

where $\mathcal{L} \equiv \sigma$ and $\mathcal{T} \equiv \lambda$. Let us define the space of weighted $L_2(\mathfrak{K})$ as in the form

$$\mathbb{Z}_V \equiv L_{2,V}(\mathfrak{K}) := \Big\{\xi : \mathfrak{K} \to \mathbb{R} : \xi \textit{ is measurable and } \|\xi(\varkappa,\varsigma)\|_V < \infty\Big\}. \tag{27}$$

Here, the weight function $V(\varkappa,\varsigma)$ is expressed as a product of two weight functions $\mathfrak{w}_{\mathcal{L}}(\varkappa)$ and $\mathfrak{w}_{\mathcal{R}}(\varsigma)$ associated with SJPs and RJPs introduced above. Specifically, we have $V(\varkappa,\varsigma) = \mathfrak{w}_{\mathcal{L}}(\varkappa)\mathfrak{w}_{\mathcal{R}}(\varsigma)$. The norm associated with this space is provided by

$$\|\mathbf{X}(\varkappa,\varsigma)\|_V := \int_0^{\mathcal{L}} \int_0^{\mathcal{T}} |\mathbf{X}(\varkappa,\varsigma)|^2 V(\varkappa,\varsigma) d\varkappa d\varsigma. \tag{28}$$

The following inner product will be considered on the space $\mathbb{Z}_V$

$$\langle \mathbf{X}, \mathbf{Y} \rangle_V := \int_0^{\mathcal{L}} \int_0^{\mathcal{T}} \mathbf{X}(\varkappa, \varsigma)\mathbf{Y}(\varkappa, \varsigma)V(\varkappa, \varsigma)d\varkappa d\varsigma. \tag{29}$$

Now, let us have a finite-dimensional subspace of $\mathbb{Z}_V$, abbreviated as $\mathbb{G}_{N,M}$, where the following hold:

$$\mathbb{G}_{N,M} := Span\Big\{\mathcal{J}_i^{\alpha,\beta}(\varkappa)\mathcal{R}_j^{\upsilon,\varepsilon}(\varsigma)|\ i = 0, 1, ..., N,\ j = 0, 1, ...M\Big\}. \tag{30}$$

It is remarked that $\mathbb{G}_{N,M}$ is a complete subspace of $\mathbb{Z}_V$.

We now assume that an element $\aleph(\varkappa, \varsigma) \in \mathbb{Z}_V$ is realized by an element in $\mathbb{G}_{N,M}$. An element $g_*(\varkappa, \varsigma) \in \mathbb{G}_{N,M}$ is said to be the best (closest) approximation of $\aleph(\varkappa, \varsigma)$ if the above relation is satisfied

$$\|\aleph - g_*\|_V = \inf_{\varrho \in \mathbb{Z}_V} \|\aleph - \varrho\|_V. \tag{31}$$

For the existence of the best approximation, refer to [[47], Thm. I1]. As a last goal, let $\widetilde{\aleph}(\varkappa, \varsigma) \in \mathbb{G}_{N,M}$ be the approximate solution of $\aleph(\varkappa, \varsigma)$ as the solution to the model problem. Then we have

$$\aleph(\varkappa, \varsigma) \approx \widetilde{\aleph}(\varkappa, \varsigma) = \sum_{i=0}^{N}\sum_{j=0}^{M} a_{ij}\mathcal{J}_i^{\alpha,\beta}(\varkappa)\mathcal{R}_j^{\upsilon,\varepsilon}(\varsigma) = \Psi_M^T(\varsigma)\mathbf{A}\Phi_N(\varkappa),\ (\varkappa, \varsigma) \in \mathfrak{K}, \tag{32}$$

where the matrix $\mathbf{A}$ is given by

$$\mathbf{A} = \begin{pmatrix} a_{00} & a_{01} & \cdots & a_{0M} \\ a_{10} & a_{11} & \cdots & a_{1M} \\ \vdots & \vdots & \ddots & \vdots \\ a_{N0} & a_{N1} & \cdots & a_{NM} \end{pmatrix}. \tag{33}$$

We will now show that the difference between $\aleph(\varkappa, \varsigma)$ and its approximation $\widetilde{\aleph}(\varkappa, \varsigma)$ approaches zero as the numbers N and M approach infinity. Thus, we introduce

$$\mathcal{I}_{N,M}(\varkappa, \varsigma) := \aleph(\varkappa, \varsigma) - \widetilde{\aleph}(\varkappa, \varsigma). \tag{34}$$

If $\Im$ is equal to N and M, then we have the error $\mathcal{I}_{\Im}(\varkappa, \varsigma)$. Here, we have the following result.

Theorem 1. *Let us consider a continuous function $\aleph : \mathfrak{K} \to \mathbb{R}$, for which we know that there exist and are continuous all partial derivatives of $\aleph(\varkappa, \varsigma)$. We also suppose that the values of all such derivatives are bounded by some constant $\mathfrak{E}$. If the representation $\widetilde{\aleph}(\varkappa, \varsigma) = \Psi_M^T(\varsigma)\mathbf{A}\Phi_N(\varkappa)$ as in (32) is the optimal (best) approximation to $\aleph(\varkappa, \varsigma)$ in $\mathbb{G}_{N,M}$ for $\Im = N = M$, we can derive that*

$$\begin{aligned}\|\mathcal{I}_{\Im}(\varkappa, \varsigma)\|_V^2 \le \frac{\mathfrak{E}^2}{\Gamma^2(1+\mathfrak{E})}\Big[&\frac{\mathcal{L}^{\alpha+\beta+1}exp(\varepsilon\mathcal{T})\mathcal{T}^{(2\Im+\upsilon+1)}}{(2\Im+\upsilon+1)} + exp(\varepsilon\mathcal{T})\mathcal{T}^{(2\Im+\upsilon+1)}exp\left(\frac{2\Im\mathcal{L}}{\mathcal{T}}\right) \\ &+ \frac{\mathcal{L}^{2\Im+\alpha+\beta+1}exp(\varepsilon\mathcal{T})\mathcal{T}^{(\upsilon+1)}}{2\Im(\upsilon+1)}\Big],\end{aligned} \tag{35}$$

then we have

$$\|\mathcal{I}_{\Im}(\varkappa, \varsigma)\|V \to 0,\ as\ \Im \to \infty. \tag{36}$$

Proof By referring to Theorem 2.2 in [48], setting $\epsilon = 1$, we obtain the desired result. □

3 Spectral Approach to Solving FitzHugh-Nagumo Nonlinear Equation (FH-NNE)

This section focuses on deriving a shifted Jacobi and Romanovski-Jacobi spectral collocation method (SJRSCM) to address the following FH-NNE of the form [4]:

$$\frac{\partial \aleph(\varkappa,\varsigma)}{\partial \varsigma} = \frac{\partial^2 \aleph(\varkappa,\varsigma)}{\partial \varkappa^2} - \aleph(\varkappa,\varsigma)(\eta - \aleph(\varkappa,\varsigma))(1-\aleph(\varkappa,\varsigma)),\ 0<\eta\leq 1, \tag{37}$$

under the initial condition

$$\aleph(\varkappa,0) = \mathcal{G}_1(\varkappa),\ 0\leq\varkappa\leq\sigma, \tag{38}$$

and the boundary conditions

$$\aleph(0,\varsigma) = \mathcal{H}_1(\varsigma), \qquad \aleph(\sigma,\varsigma) = \mathcal{H}_2(\varsigma),\ 0\leq\varsigma\leq\lambda, \tag{39}$$

where $\mathcal{G}_1(\varkappa)$, $\mathcal{H}_1(\varsigma)$ and $\mathcal{H}_2(\varsigma)$ are given functions. To advance with the proposed numerical algorithm, we approximate the following functions: $\frac{\partial \aleph(\varkappa,\varsigma)}{\partial \varsigma}$ and $\frac{\partial^2 \aleph(\varkappa,\varsigma)}{\partial \varkappa^2}$ as expansions in the SJPs and RJPs as

$$\frac{\partial \widetilde{\aleph}(\varkappa,\varsigma)}{\partial \varsigma} = \sum_{i=0}^{N}\sum_{j=0}^{M} a_{ij}\mathcal{J}_i^{\alpha,\beta}(\varkappa)\frac{\partial \mathcal{R}_j^{\upsilon,\varepsilon}(\varsigma)}{\partial \varsigma} = \Theta^{(1)}\Psi_M^T(\varsigma)\mathbf{A}\Phi_N(\varkappa), \tag{40}$$

$$\frac{\partial^2 \widetilde{\aleph}(\varkappa,\varsigma)}{\partial \varkappa^2} = \sum_{i=0}^{N}\sum_{j=0}^{M} a_{ij}\frac{\partial^2 \mathcal{J}_i^{\alpha,\beta}(\varkappa)}{\partial \varkappa^2}\mathcal{R}_j^{\upsilon,\varepsilon}(\varsigma) = \Psi_M^T(\varsigma)\mathbf{A}\Delta^{(2)}\Phi_N(\varkappa). \tag{41}$$

By utilizing the series of equations (32), (40) and (41), we can derive the following approximations:

$$\Theta^{(1)}\Psi_M^T(\varsigma)\mathbf{A}\Phi_N(\varkappa) = \Psi_M^T(\varsigma)\mathbf{A}\Delta^{(2)}\Phi_N(\varkappa) - \Psi_M^T(\varsigma)\mathbf{A}\Phi_N(\varkappa)(\eta - \Psi_M^T(\varsigma)\mathbf{A}\Phi_N(\varkappa)).\quad 0\leq\varkappa\leq\sigma,\ 0\leq\varsigma\leq\lambda. \tag{42}$$

Furthermore, the conditions specified in (38) and (39) lead to the following equations:

$$\Psi_M^T(0)\mathbf{A}\Phi_N(\varkappa) \approx \mathcal{G}_1(\varkappa), \tag{43}$$

$$\Psi_M^T(\varsigma)\mathbf{A}\Phi_N(0) \approx \mathcal{H}_1(\varsigma), \tag{44}$$

$$\Psi_M^T(\varsigma)\mathbf{A}\Phi_N(\sigma) \approx \mathcal{H}_2(\varsigma). \tag{45}$$

With the collocation procedure, we can now solve Eqs. (42)–(45). Suppose $\varsigma_j^{\upsilon,\varepsilon}$, $j=0,1,\cdots,M$ are the zeros of $\mathcal{R}_{M+1}^{\upsilon,\varepsilon}(\varsigma)$, while $\varkappa_i^{\alpha,\beta}$, $i=0,1,\cdots,N$ are the zeros of $\mathcal{J}_{N+1}^{\alpha,\beta}(\varkappa)$. We substitute these nodes into (42)–(45). Accordingly, we have

$$\Theta^{(1)}\Psi_M^T(\varsigma_j^{\upsilon,\varepsilon})\mathbf{A}\Phi_N(\varkappa_i^{\alpha,\beta}) = \Psi_M^T(\varsigma_j^{\upsilon,\varepsilon})\mathbf{A}\Delta^{(2)}\Phi_N(\varkappa_i^{\alpha,\beta}) - \Psi_M^T(\varsigma_j^{\upsilon,\varepsilon})\mathbf{A}\Phi_N(\varkappa_i^{\alpha,\beta})(\eta - \Psi_M^T(\varsigma_j^{\upsilon,\varepsilon})\mathbf{A}\Phi_N(\varkappa_i^{\alpha,\beta})),\quad 1\leq i\leq N-1,\ 0\leq j\leq M-1, \tag{46}$$

$$\Psi_M^T(0)\mathbf{A}\Phi_N(\varkappa_i^{\alpha,\beta}) = \mathcal{G}_1(\varkappa_i^{\alpha,\beta}),\ 0\leq i\leq N, \tag{47}$$

$$\Psi_M^T(\varsigma_j^{\upsilon,\varepsilon})\mathbf{A}\Phi_N(0) = \mathcal{H}_1(\varsigma_j^{\upsilon,\varepsilon}),\ 0\leq j\leq M-1, \tag{48}$$

$$\Psi_M^T(\varsigma_j^{\upsilon,\varepsilon})\mathbf{A}\Phi_N(\sigma) = \mathcal{H}_2(\varsigma_j^{\upsilon,\varepsilon}),\ 0\leq j\leq M-1. \tag{49}$$

This approach yields an algebraic system of $(N+1)\times(M+1)$ equations, which can be solved using any appropriate iterative algorithm, such as Newton's method. Consequently, the approximate solution $\widetilde{\aleph}(\varkappa,\varsigma)$ can be determined.

Remark 3: *Section 4 outlines the computational algorithm employed to solve various numerical examples. The computations were performed on an Intel(R) Core(TM) i9-10850 CPU operating at* 3.60 *GHz, featuring* 10 *cores and* 20 *logical processors, utilizing Mathematica* 11.3.0*. The shifted Jacobi and Romanovski-Jacobi spectral collocation method was implemented, and the following algorithmic steps in Algorithm 1 were applied to solve the FitzHugh-Nagumo nonlinear equation:*

Algorithm 1: Computational algorithm for solving the FitzHugh-Nagumo nonlinear equation

Step 1. Given $\alpha,\ \beta,\ \upsilon,\ \varepsilon,\ \sigma,\ \lambda,\ \mathcal{G}_1(\varkappa),\ \mathcal{H}_1(\varsigma)$ and $\mathcal{H}_2(\varsigma)$.

Step 2. Define the basis functions of the SJPs $\mathcal{J}_i^{\alpha,\beta}(\varkappa)$, RJPs $\mathcal{R}_j^{\upsilon,\varepsilon}(\varsigma)$ and the matrices $\mathbf{A},\ \Psi_M^T(\varsigma)$, $\Phi_N(\varkappa),\ \Theta^{(1)}$ and compute $\Delta^{(2)}$.

Step 3. Evaluate the matrices:
1. $\Psi_M^T(\varsigma)\mathbf{A}\Phi_N(\varkappa)$,
2. $\Theta^{(1)}\Psi_M^T(\varsigma)\mathbf{A}\Phi_N(\varkappa)$,
3. $\Psi_M^T(\varsigma)\mathbf{A}\Delta^{(2)}\Phi_N(\varkappa)$.

Step 4. Using Eqs. (32), (40) and (41) to get the matrix form of Eqs. (42)–(45).

Step 5. Apply the collocation method to obtain a system of equations as in (46)–(49).

Step 6. Use FindRoot command in Mathematica, which employs Newton's method, with an initial guess $\{a_{ij} = 10^{-i-j},\ i : 0, 1, \ldots, N,\ j : 0, 1, \ldots, M\}$ to solve the system (46)–(49) to get a_{ij}.

Step 7. Compute $\widetilde{\aleph}(\varkappa, \varsigma)$ defined in Eq. (32).

4 Numerical Results

To demonstrate the efficacy of the proposed method, this section presents several numerical examples. A comparative analysis of the results obtained using the proposed method against those derived from alternative approaches underscores the method's high efficiency and practicality. The accuracy of the results is evaluated using the absolute error, defined as

$$E(\varkappa, \varsigma) = |\aleph(\varkappa, \varsigma) - \widetilde{\aleph}(\varkappa, \varsigma)|,\ (\varkappa, \varsigma) \in \mathfrak{K},$$

where $\aleph(\varkappa, \varsigma)$ and $\aleph_N(\varkappa, \varsigma)$ are the exact solution and the numerical solution at the point $(\varkappa, \varsigma)$, respectively, and the following maximum absolute errors (MAEs)

$$MAEs = Max\{E(\varkappa, \varsigma) : \forall(\varkappa, \varsigma) \in [0, \sigma] \times [0, \lambda]\}.$$

The following examples are considered.

Example 1. *([4]), we consider the following nonlinear FitzHugh-Nagumo equation in the form:*

$$D_\varsigma \aleph = D_{\varkappa\varkappa}\aleph - \aleph(\eta - \aleph)(1 - \aleph),\ 0 < \eta \leq 1, \tag{50}$$

under the initial condition

$$\aleph(\varkappa, 0) = \frac{\eta\lambda e^{\frac{\eta\varkappa}{\sqrt{2}}} + \mu e^{\frac{\varkappa}{\sqrt{2}}}}{\eta\lambda e^{\frac{\eta\varkappa}{\sqrt{2}}} + \mu e^{\frac{\varkappa}{\sqrt{2}}} + \sigma},\ 0 < \varkappa \leq 1, \tag{51}$$

and the boundary conditions

$$\begin{aligned}\aleph(0,\varsigma) &= \frac{\eta\lambda e^{\frac{\eta^2\varsigma}{2}} + \mu e^{\frac{\varsigma}{2}}}{\eta\lambda e^{\frac{\eta^2\varsigma}{2}} + \sigma e^{\eta\varsigma} + \mu e^{\frac{\varsigma}{2}}},\ 0 < \varsigma \le 1,\\ \aleph(1,\varsigma) &= \frac{\eta\lambda e^{\frac{1}{2}\eta(\eta\varsigma+\sqrt{2})} + \mu e^{\frac{1}{2}(\varsigma+\sqrt{2})}}{\eta\lambda e^{\frac{1}{2}\eta(\eta\varsigma+\sqrt{2})} + \sigma e^{\eta\varsigma} + \mu e^{\frac{1}{2}(\varsigma+\sqrt{2})}},\ 0 < \varsigma \le 1,\end{aligned} \tag{52}$$

where $\eta,\ \mu,\ \sigma$ *are constants and* $\aleph(\varkappa,\varsigma) = \dfrac{\mu e^{(\frac{1}{2}-\eta)\varsigma+\frac{\sqrt{2}\varkappa}{2}} + \eta\lambda e^{(\frac{\eta}{2}-1)\eta\varsigma+\frac{\sqrt{2}\varkappa}{2}}}{\mu e^{(\frac{1}{2}-\eta)\varsigma+\frac{\sqrt{2}\varkappa}{2}} + \eta\lambda e^{(\frac{\eta}{2}-1)\eta\varsigma+\frac{\sqrt{2}\varkappa}{2}} + \sigma}$ *is the exact solution of this problem.*

Table 1 provides a comparison of the absolute errors for solving Example 1 at $t = 1$ *using the SJRSCM and the results reported by Shekarabi et al. [4]. The data demonstrate that the SJRSCM achieves significantly higher accuracy, particularly for* $\upsilon = 2$ *and* $\varepsilon = -35$*, which produce the smallest absolute errors. Furthermore, the performance at* $\upsilon = 3$ *and* $\upsilon = 4$ *also highlights the robustness of the method under varying parameters. These results confirm the effectiveness of SJRSCM in addressing numerical challenges and reducing errors. Table 2 illustrates the absolute errors of the exact solution and the numerical solution for Example 1 under various parameter settings. The results reveal that increasing* υ *and adjusting* ε *significantly affect the error levels, with* $\upsilon = 1$ *and* $\varepsilon = -30$ *achieving the lowest error magnitudes. As* υ *and* ε *vary, the error remains relatively low, demonstrating the stability and accuracy of the numerical method. These findings validate the method's capability to produce precise approximations for different scenarios, highlighting its robustness in solving complex numerical problems. Table 3 compares the absolute errors (AE) and CPU times for different values of* $\alpha = \beta$ *and* υ *with specified* ε*. The results demonstrate that the absolute errors decrease as the values of* α *and* β *vary, while the CPU times exhibit significant fluctuations across the tested scenarios. These findings, as illustrated in Example 1, offer valuable insights into the algorithm's performance under varying conditions, contributing to the enhancement of computational efficiency and accuracy. Fig. 1 presents the space-time graphs of the approximate solution (left) and the absolute error function (right) for Example 1 with* $\alpha = \beta = 0, \upsilon = 5,$ $\varepsilon = -60$*, and* $N = M = 7$*. The graph on the left illustrates a smooth and accurate approximation of the solution as values change. On the right, the graph shows the distribution of the absolute error, which remains at low levels, reflecting the efficiency of the method in minimizing errors and achieving high accuracy.*

Table 1: Comparison of the absolute errors for Example 1 at $t = 1$

	Shekarabi et al. [4]	SJRSCM ($\alpha = \frac{1}{2},\ \beta = -\frac{1}{2},\ N = M = 7$)		
$\varkappa$		$\upsilon = 2,\ \varepsilon = -35$	$\upsilon = 3,\ \varepsilon = -45$	$\upsilon = 4,\ \varepsilon = -40$
0.1	1.41366×10^{-6}	3.30018×10^{-9}	1.79685×10^{-8}	3.54448×10^{-8}
0.2	1.39287×10^{-6}	2.45260×10^{-8}	2.74514×10^{-8}	8.25325×10^{-9}
0.3	1.18067×10^{-6}	2.04282×10^{-8}	3.97077×10^{-8}	2.27489×10^{-8}
0.4	1.16488×10^{-6}	4.61135×10^{-8}	2.0923×10^{-8}	1.65177×10^{-8}
0.5	8.85464×10^{-7}	8.08998×10^{-8}	6.14507×10^{-8}	5.73337×10^{-8}
0.6	9.60502×10^{-7}	7.14577×10^{-8}	1.36604×10^{-7}	7.31018×10^{-9}

(Continued)

Table 1 (continued)

	Shekarabi et al. [4]	SJRSCM ($\alpha = \frac{1}{2}$, $\beta = -\frac{1}{2}$, $N = M = 7$)		
$\varkappa$		$\upsilon = 2,\ \varepsilon = -35$	$\upsilon = 3,\ \varepsilon = -45$	$\upsilon = 4,\ \varepsilon = -40$
0.7	5.91894×10^{-7}	4.18585×10^{-7}	6.92969×10^{-8}	1.94768×10^{-7}
0.8	7.75841×10^{-7}	5.29278×10^{-7}	5.23185×10^{-8}	2.41736×10^{-7}
0.9	3.12309×10^{-7}	7.74905×10^{-7}	$1.56639. \times 10^{-7}$	5.55958×10^{-7}

Table 2: Absolute error of the the exact solution and the numerical solution for Example 1 at $N = M = 7, \eta = 1, \mu = 3, \lambda = 2, \sigma = 4, \alpha = \beta = \frac{1}{2}$

$\varkappa$	ς	$\upsilon = 1,\ \varepsilon = -30$	$\upsilon = 4,\ \varepsilon = -60$	$\upsilon = 5,\ \varepsilon = -60$
0.2	0.3	6.0700×10^{-10}	4.1599×10^{-8}	9.5648×10^{-8}
	0.6	4.1523×10^{-10}	3.4916×10^{-8}	7.2944×10^{-8}
	0.9	2.2669×10^{-12}	1.8374×10^{-8}	2.8068×10^{-8}
0.4	0.3	1.1823×10^{-9}	8.2778×10^{-8}	1.8973×10^{-7}
	0.6	7.2201×10^{-10}	6.6932×10^{-8}	1.3863×10^{-7}
	0.9	8.2542×10^{-10}	3.0737×10^{-8}	4.3954×10^{-8}
0.6	0.3	2.0084×10^{-9}	1.2336×10^{-7}	2.7982×10^{-7}
	0.6	1.3782×10^{-9}	9.2785×10^{-8}	1.8865×10^{-7}
	0.9	8.7491×10^{-10}	2.9899×10^{-8}	3.7743×10^{-8}
0.8	0.3	6.0113×10^{-9}	1.5473×10^{-7}	3.3522×10^{-7}
	0.6	5.4536×10^{-9}	1.0474×10^{-7}	2.0244×10^{-7}
	0.9	1.1215×10^{-8}	2.9741×10^{-8}	6.8642×10^{-8}

Table 3: Comparison of absolute errors (AE) and CPU times for different values of $\alpha = \beta$ and υ with specified ε for Example 1 at $N = M = 6$

$\alpha = \beta$	$\upsilon = 1,\ \varepsilon = -40$		$\upsilon = 2,\ \varepsilon = -50$	
	AE	CPU time	AE	CPU time
$-\frac{1}{2}$	3.4506×10^{-6}	200.36	3.2660×10^{-5}	217.422
0	1.6795×10^{-6}	227.109	1.5881×10^{-5}	213.845
$\frac{1}{2}$	1.2847×10^{-6}	168.234	1.0482×10^{-5}	149.156

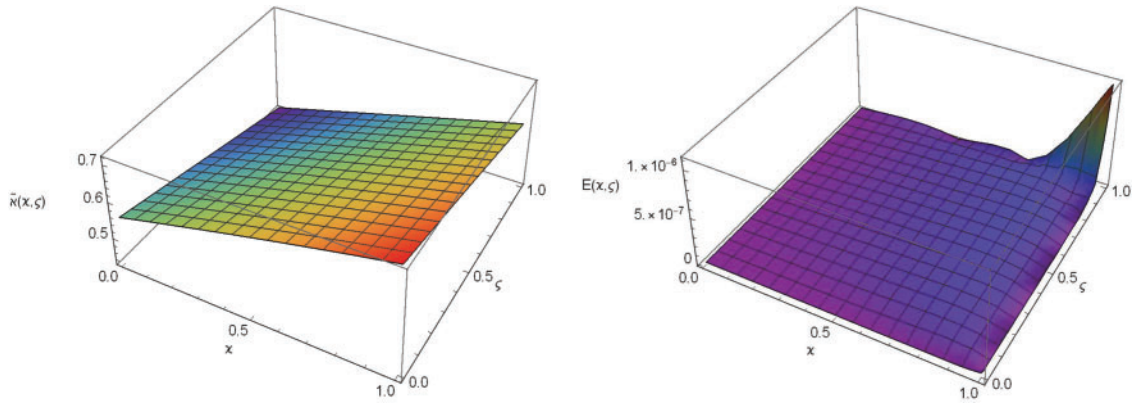

Figure 1: The space-time graphs of the approximate solution (left)and its absolute error function (right) for Example 1 with $\alpha = \beta = 0,\ \upsilon = 5,\ \varepsilon = -60$ and $N = M = 7$

Example 2: *Consider the nonlinear FitzHugh-Nagumo equation (see [3]):*

$$D_{\varsigma}\aleph = D_{\varkappa\varkappa}\aleph - \aleph(\eta - \aleph)(1 - \aleph),\ 0 < \eta \leq 1, \tag{53}$$

under the initial condition

$$\aleph(\varkappa, 0) = \frac{e^{-\frac{\varkappa}{\sqrt{2}}}}{-e^{-\frac{\varkappa}{\sqrt{2}}} - 2} + 1,\ 0 < \varkappa \leq 1, \tag{54}$$

and the boundary conditions

$$\aleph(0, \varsigma) = \frac{2}{e^{\frac{\varsigma}{2}} + 2}, \quad \aleph(1, \varsigma) = \frac{2e^{\frac{1}{\sqrt{2}}}}{e^{\frac{\varsigma}{2}} + 2e^{\frac{1}{2}}}, \quad 0 < \varsigma \leq 1, \tag{55}$$

where $\aleph(\varkappa, \varsigma) = \dfrac{e^{\frac{\varsigma}{2} - \frac{\varkappa}{\sqrt{2}}}}{-e^{\frac{\varsigma}{2} - \frac{\varkappa}{\sqrt{2}}} - 2} + 1$ *is the exact solution of this problem when* $\eta = 1$.

Table 4 provides an accurate comparison of the absolute errors resulting from the finite forward difference method (Yokus [3]) and the new SJRSCM in Example 2 at time $t = 0.001$. *The table presents the absolute error values for small variations in the parameter* $\varkappa$ *(ranging from* 0.000 *to* 0.006*) and compares the methods based on the parameters* $\alpha = \beta = \dfrac{1}{2}$, $N = M = 7$, with different values of υ and ε. *These results highlight that the adjustments in the values of* υ *and* ε *in the new method lead to substantial improvements in accuracy, making it suitable for applications requiring high precision with small variations in* $\varkappa$. *Table 5 presents a comparison of the absolute errors for two different methods used to solve a numerical example at a specific time* $t = 0.001$. *The first method is Abd-Elhameed et al. [49] approach using the collocation method with* $N = 9$, *while the second method is SJRSCM with specific parameters* ($\upsilon = 4,\ \varepsilon = -55,\ N = M = 7$) *and three different cases for the values of* α and β. *From the table, it can be observed that the SJRSCM method yields lower absolute errors compared to Abd-Elhameed et al. [49] method in all the mentioned cases. This suggests that SJRSCM may be more accurate in this specific numerical context. Furthermore, the results show that varying the values of* α *and* β *in the SJRSCM method has a slight impact on the accuracy of the results, as the absolute errors remain within a close range. This may indicate the method's flexibility and its ability to maintain accuracy under different conditions. Table 6 shows the absolute error between the exact solution and the numerical solution for Example 2 with* $N = M = 7$ *and* $\alpha = \beta = 0$. *The table compares the error values for*

different combinations of $\upsilon = 2, 3, 4$ *and* $\varepsilon = -35, -45, -55$ *over various values of* $\varkappa = \varsigma$ *ranging from* 0.1 *to* 0.9. *The results indicate that the numerical method achieves a high level of accuracy, with errors remaining very small across all parameters. Notably, the absolute error increases slightly as* κ *increases, and higher values of* ν *and* ϵ *generally result in larger errors, although still within acceptable limits. Fig. 2 illustrates the comparison between the analytical solutions and the approximate solutions for Example 2 at* $\varsigma = 0.2, 0.6, 1$. *The left plot shows the variation with* $\varkappa$, *while the right plot presents the variation with* ς. *The parameters used are* $\alpha = \beta = \frac{1}{2}$, $\upsilon = 2$, $\varepsilon = -35$, and $N = M = 7$. *It is observed that the approximate solutions* ($\widetilde{\aleph}$) *closely match the analytical solutions* ($\aleph$), *highlighting the efficiency of the numerical method employed. The similarity between the curves demonstrates the accuracy of the approximate solutions across different values of* ς *and* $\varkappa$.

Table 4: Comparison of the absolute errors for Example 2 at $t = 0.001$

	Yokus	SJRSCM ($\alpha = \beta = \frac{1}{2}$, $N = M = 7$)		
$\varkappa$	[3]	$\upsilon = 3$, $\varepsilon = -40$	$\upsilon = 4$, $\varepsilon = -60$	$\upsilon = 5$, $\varepsilon = -80$
0.00	$9.26009136074645 \times 10^{-9}$	5.12690×10^{-12}	2.75845×10^{-12}	4.44528×10^{-13}
0.001	$9.26694588350983 \times 10^{-9}$	4.82378×10^{-12}	2.77009×10^{-12}	9.95574×10^{-13}
0.002	$9.273449896873842 \times 10^{-9}$	4.54138×10^{-12}	2.79327×10^{-12}	1.54950×10^{-12}
0.003	$9.279814694451716 \times 10^{-9}$	4.27872×10^{-12}	2.82772×10^{-12}	2.10591×10^{-12}
0.004	$9.286474367264930 \times 10^{-9}$	4.03514×10^{-12}	2.87178×10^{-12}	2.66475×10^{-12}
0.005	$9.292864144860857 \times 10^{-9}$	3.80994×10^{-12}	2.92634×10^{-12}	3.22588×10^{-12}
0.006	$9.299528924699985 \times 10^{-9}$	3.60232×10^{-12}	2.99047×10^{-12}	3.78907×10^{-12}

Table 5: Comparison of the absolute errors for Example 2 at $t = 0.001$

	Abd-Elhameed et al.	SJRSCM ($\upsilon = 4$, $\varepsilon = -55$, $N = M = 7$)		
$\varkappa$	[49] (N = 9)	$\alpha = \frac{1}{2}$, $\beta = -\frac{1}{2}$	$\alpha = \beta = 0$	$\alpha = -\frac{1}{2}$, $\beta = \frac{1}{2}$
0.00	1.5309×10^{-11}	6.0125×10^{-12}	6.4881×10^{-12}	6.1176×10^{-12}
0.001	1.4873×10^{-11}	5.6093×10^{-12}	6.1326×10^{-12}	6.2637×10^{-12}
0.002	1.4446×10^{-11}	5.2275×10^{-12}	5.7988×10^{-12}	5.9375×10^{-12}
0.003	1.3624×10^{-11}	4.8660×10^{-12}	5.48660×10^{-12}	5.6323×10^{-12}
0.004	1.3624×10^{-11}	4.5242×10^{-12}	5.1929×10^{-12}	5.3473×10^{-12}
0.005	1.3227×10^{-11}	4.2014×10^{-12}	4.9193×10^{-12}	5.0817×10^{-12}
0.006	1.2840×10^{-11}	3.8968×10^{-12}	4.6643×10^{-12}	4.8350×10^{-12}

Table 6: Absolute error of the the exact solution and the numerical solution for Example 2 at $N = M = 7$, $\alpha = \beta = 0$

$\varkappa = \varsigma$	$\upsilon = 2,\ \varepsilon = -35$	$\upsilon = 3,\ \varepsilon = -45$	$\upsilon = 4,\ \varepsilon = -55$
0.1	7.0439×10^{-11}	1.3378×10^{-10}	1.4678×10^{-9}
0.2	7.1100×10^{-10}	9.1721×10^{-10}	8.8112×10^{-9}
0.3	1.8969×10^{-9}	2.1888×10^{-9}	1.9472×10^{-8}
0.4	3.5205×10^{-9}	3.7891×10^{-9}	3.2264×10^{-8}
0.5	5.6866×10^{-9}	5.9335×10^{-9}	4.8795×10^{-8}
0.6	8.5178×10^{-9}	8.0885×10^{-9}	6.5474×10^{-8}
0.7	1.2978×10^{-8}	1.1060×10^{-8}	8.2134×10^{-8}
0.8	1.6937×10^{-8}	1.6372×10^{-8}	9.8604×10^{-8}
0.9	1.6764×10^{-8}	1.8070×10^{-8}	8.4206×10^{-8}

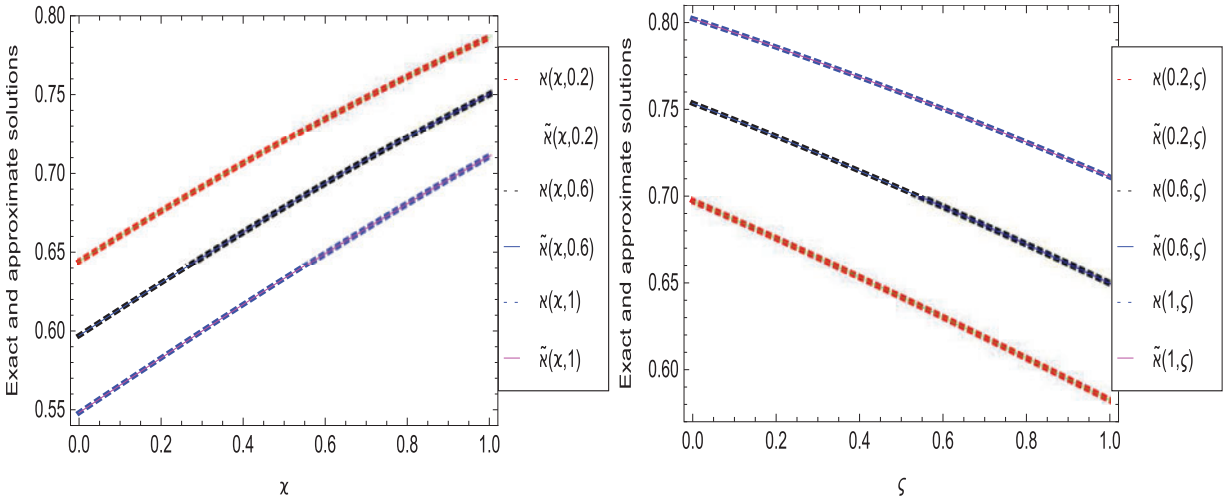

Figure 2: The comparison of the curves of analytical solutions and approximate solutions at $\varsigma = 0.2,\ 0.6,\ 1$ (left) and $\varkappa = 0.2,\ 0.6,\ 1$ (right) for Example 2 with $\alpha = \beta = \frac{1}{2},\ \upsilon = 2,\ \varepsilon = -35$ and $N = M = 7$

Example 3: *Consider the nonlinear FitzHugh-Nagumo equation (see [7]):*

$$D_{\varsigma}\aleph = D_{\varkappa\varkappa}\aleph - \aleph(\eta - \aleph)(1 - \aleph),\ 0 < \eta \leq 1, \tag{56}$$

under the initial condition

$$\aleph(\varkappa, 0) = \frac{1}{2}\tanh\left(\frac{\varkappa}{2\sqrt{2}}\right) + \frac{1}{2},\ 0 < \varkappa \leq 1, \tag{57}$$

and the boundary conditions

$$\aleph(0,\varsigma) = \frac{1}{2} - \frac{1}{2}\tanh\left(\frac{1}{4}(2\eta-1)\varsigma\right), \quad 0 < \varsigma \le 1,$$

$$\aleph(1,\varsigma) = \frac{1}{2}\tanh\left(\frac{1-\frac{(2\eta-1)\varsigma}{\sqrt{2}}}{2\sqrt{2}}\right) + \frac{1}{2}, \quad 0 < \varsigma \le 1, \tag{58}$$

where $\aleph(\varkappa,\varsigma) = \frac{1}{2}\tanh\left(\frac{\varkappa-\frac{(2\eta-1)\varsigma}{\sqrt{2}}}{2\sqrt{2}}\right) + \frac{1}{2}$ *is the exact solution of this problem.*

Table 7 presents the absolute error between the exact solution and the numerical solution for Example 3 at $\eta = \frac{1}{2}$, $\alpha = \beta = \frac{1}{2}$ *and* $N = M = 7$. *The data shows that the absolute error gradually increases as* $\varkappa = \varsigma$ *increases. Additionally, the effect of varying* υ *and* ε *on the accuracy of the solution is noticeable, where the error increases with larger values of* υ *and smaller values of* ε. *This indicates that the numerical solution is more accurate for smaller values of* $\varkappa$, *and accuracy decreases as the parameters increase. Fig. 3 shows a comparison between the analytical and approximate solutions for different values of* ς *and* $\varkappa(0.3,\ 0.6,$ *and* $0.9)$. *The left graph demonstrates the solutions as a function of* $\varkappa$, *where the approximate solutions closely follow the analytical ones. Similarly, the right graph displays the solutions as a function of* ς, *confirming the accuracy of the numerical method. The graphs highlight that the numerical solutions remain in good agreement with the exact solutions across the tested parameter values, with slight deviations observed as* ς *and* $\varkappa$ *increase. Fig. 4 illustrates the space-time graphs of the approximate solution (left) and its absolute error function (right) for Example 3 with parameters* $\alpha = \beta = 0$, $\upsilon = 1$, $\varepsilon = -30$, *and* $N = M = 7$. *The left graph demonstrates the smooth and accurate approximation of the solution, while the right graph highlights the distribution of the absolute error, which remains at low levels across the domain. This confirms the effectiveness of the proposed method in achieving high accuracy and minimizing computational errors for the FitzHugh-Nagumo equation under the given conditions.*

Table 7: Absolute error of the exact solution and the numerical solution for Example 3 at $\eta = \frac{1}{2}$, $\alpha = \beta = \frac{1}{2}$ and $N = M = 7$

$\varkappa = \varsigma$	$\upsilon = 2,\ \varepsilon = -35$	$\upsilon = 3,\ \varepsilon = -45$	$\upsilon = 4,\ \varepsilon = -55$
0.1	5.2617×10^{-10}	3.9509×10^{-10}	2.8238×10^{-9}
0.2	2.9879×10^{-9}	2.2467×10^{-9}	1.4696×10^{-8}
0.3	5.5498×10^{-9}	4.2730×10^{-9}	2.7154×10^{-8}
0.4	7.7550×10^{-9}	5.9302×10^{-9}	3.7794×10^{-8}
0.5	1.0294×10^{-8}	8.1049×10^{-9}	5.0792×10^{-8}
0.6	1.2379×10^{-8}	9.2091×10^{-9}	5.9315×10^{-8}
0.7	1.6677×10^{-8}	1.0927×10^{-8}	6.6011×10^{-8}

(Continued)

Table 7 (continued)

$\varkappa = \varsigma$	$\upsilon = 2,\ \varepsilon = -35$	$\upsilon = 3,\ \varepsilon = -45$	$\upsilon = 4,\ \varepsilon = -55$
0.8	2.1335×10^{-8}	1.4772×10^{-8}	7.7284×10^{-8}
0.9	1.5715×10^{-8}	1.1499×10^{-8}	5.7768×10^{-8}

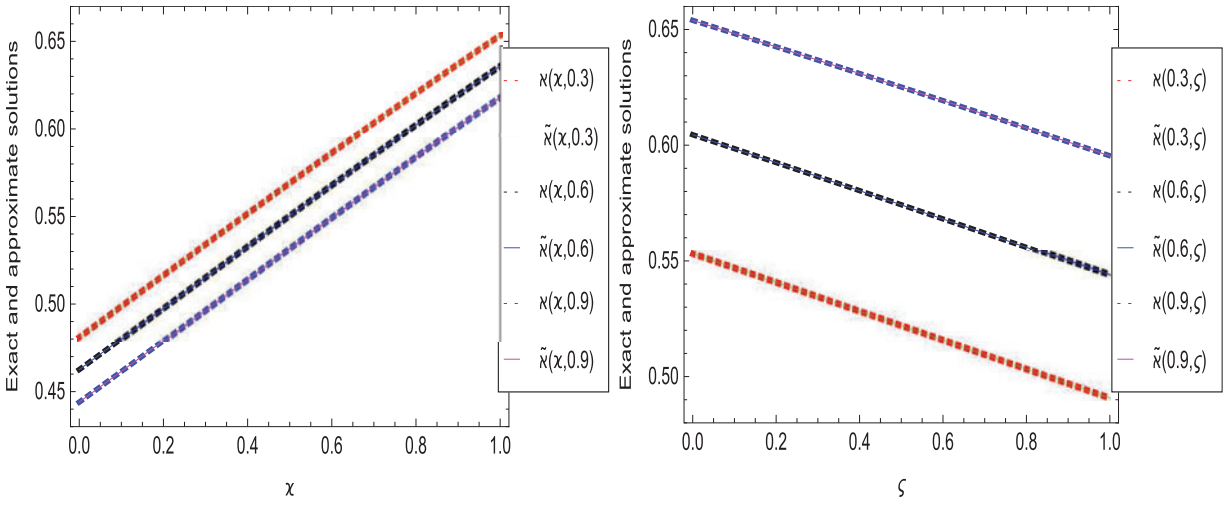

Figure 3: The comparison of the curves of analytical solutions and approximate solutions at $\varsigma = 0.3,\ 0.6,\ 0.9$ (left) and $\varkappa = 0.3,\ 0.6,\ 0.9$ (right) for Example 3 with $\eta = \frac{3}{4},\ \alpha = \beta = \frac{1}{2},\ \upsilon = 1,\ \varepsilon = -30$ and $N = M = 7$

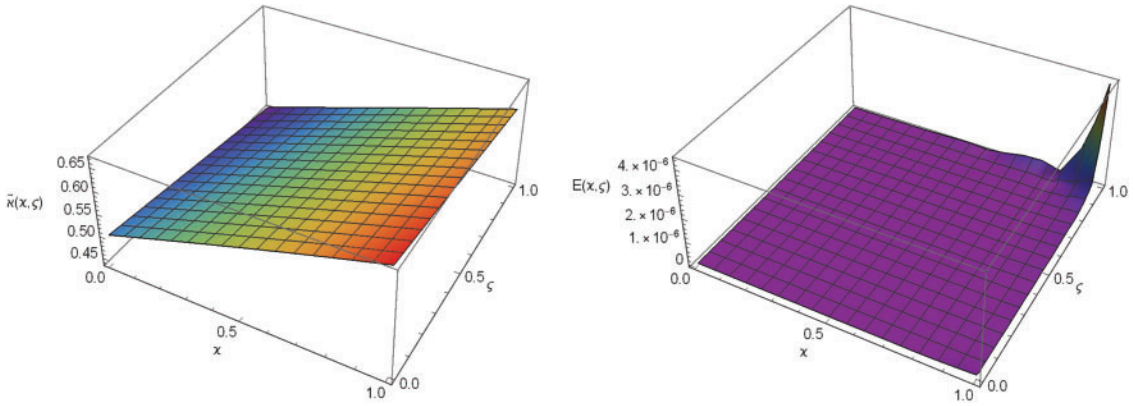

Figure 4: The space-time graphs of the approximate solution (left)and its absolute error function (right) for Example 3 with $\alpha = \beta = 0,\ \upsilon = 1,\ \varepsilon = -30$ and $N = M = 7$

5 Conclusions

In solving the FitzHugh-Nagumo problem, a new numerical framework using Jacobi and Romanovski-Jacobi polynomials is proposed. The proposed method proved to be very accurate and efficient for modeling and solving nonlinear systems, owing to the combination of spectral approaches with operational matrices. In terms of accuracy and computational time expenses, the constructed framework has overtaken conventional numerical approaches. Results indicate that the present findings may prove useful in various scientific areas, including cardiac modeling and neuroscience. Future studies may also broaden this approach to tackle other, more complex systems and equations. Research on polynomial parameter optimization should likewise develop the method's efficacy and flexibility. Moreover, its application to other nonlinear PDEs, for instance, the Burgers' or Korteweg-de Vries equation, constitutes a promising area for future research. This extension will be addressed in our upcoming studies to further confirm the generality of the proposed methodology.

Acknowledgement: The researchers would like to thank the Deanship of Graduate Studies and Scientific Research at Qassim University for financial support (QU-APC-2025).

Funding Statement: This study was financially supported by the Deanship of Graduate Studies and Scientific Research at Qassim University for financial support (QU-APC-2025).

Author Contributions: The authors confirm contribution to the paper as follows: study conception and design: Ramy Hafez; data collection: Salah Boulaaras, Hamiden Abd El-Wahed Khalifa; analysis and interpretation of results: Ramy Hafez, Salah Boulaaras, Hamiden Abd El-Wahed Khalifa; draft manuscript preparation: Ramy Hafez, Salah Boulaaras. All authors reviewed the results and approved the final version of the manuscript.

Availability of Data and Materials: All data generated or analyzed during this study are included in this published article.

Ethics Approval: Not applicable.

Conflicts of Interest: The authors declare no conflicts of interest to report regarding the present study.

References

1. Andrews GE, Askey R, Roy R. Special functions. Cambridge: Cambridge University Press; 1999.
2. Doha EH. On the construction of recurrence relations for the expansion and connection coefficients in series of Jacobi polynomials. J Phys A Math Gen. 2004;37:657–75. doi:10.1088/0305-4470/37/3/010.
3. Yokus A. On the exact and numerical solutions to the FitzHugh-Nagumo equation. Int J Mod Phys B. 2020;34:2050149. doi:10.1142/S0217979220501490.
4. Shekarabi HS, Aqamohamadi M, Rashidinia J. Tension spline method for solution of FitzHugh-Nagumo equation. Trans A Razmadze Math Instita. 2018;172(3):571–81. doi:10.1016/j.trmi.2018.02.001.
5. Youssri YH, Zaky MA, Hafez RM. Romanovski-Jacobi spectral schemes for high-order differential equations. Appl Numer Math. 2024;198:148–59. doi:10.1016/j.apnum.2023.12.015.
6. Izadi M, Veeresha P, Adel W. The fractional-order marriage-divorce mathematical model: numerical investigations and dynamical analysis. Eur Phys J Plus. 2024;139:205. doi:10.1140/epjp/s13360-024-04986-7.
7. Bhrawy AH. A Jacobi-Gauss-Lobatto collocation method for solving generalized FitzHugh-Nagumo equation with time-dependent coefficients. Appl Math Comput. 2013;222:255–64. doi:10.1016/j.amc.2013.07.056.

8. Masjedjamei M. Three finite classes of hypergeometric orthogonal polynomials and their application in functions approximation. Integral Transforms Spec Funct. 2002;13(2):169–90. doi:10.1080/10652460212898.
9. Luke Y. The special functions and their approximations, Vol. 2. New York: Academic Press; 1969.
10. Doha EH, Bhrawy AH, Hafez RM, Abdelkawy MA. A Chebyshev-Gauss-Radau scheme for nonlinear hyperbolic system of first order. Appl Math Inf Sci. 2014;8(2):1–10. doi:10.12785/amis/080211.
11. Doha EH, Bhrawy AH, Abdelkawy MA, Hafez RM. A Jacobi collocation approximation for nonlinear coupled viscous Burgers' equation. Cent Eur J Phys. 2014;12:111–22. doi:10.2478/s11534-014-0429-z.
12. Doha EH, Bhrawy AH, Hafez RM, Gorder RAV. Jacobi rational-Gauss collocation method for Lane-Emden equations of astrophysical significance. Nonlinear Anal Model. 2014;19:537–50. doi:10.15388/NA.2014.4.1.
13. Hossan MD, Datta T, Islam MD. Combining approach of collocation and finite difference methods for fractional parabolic PDEs. Partial Differ Equ Appl Math. 2024;12(21):100921. doi:10.1016/j.padiff.2024.100921.
14. Tan M, Cheng J, Shu CW. High order finite difference scheme with explicit-implicit-null time-marching for the compressible Navier-Stokes equations. J Comput Phys. 2025;523:113626. doi:10.1016/j.jcp.2024.113626.
15. Hao W, Lee S, Lee YJ. Companion-based multi-level finite element method for computing multiple solutions of nonlinear differential equations. Comput Math with Appl. 2024;168:162–73. doi:10.1016/j.camwa.2024.05.035.
16. Zhao Z, Zheng Y. A Galerkin finite element method for the space Hadamard fractional partial differential equation. Math Comput Simul. 2023;214:272–89. doi:10.1016/j.matcom.2023.06.022.
17. Trefethen LN. Spectral methods in MATLAB. UK: Oxford University Mathematical Institute; 2000.
18. Khader MM. On the numerical solutions for the fractional diffusion equation. Commun Nonlinear Sci Numer Simul. 2011;218:3925–36. doi:10.1016/j.cnsns.2010.09.007.
19. Hafez RM. Numerical solution of linear and nonlinear hyperbolic telegraph type equations with variable coefficients using shifted Jacobi collocation method. Comp Appl Math. 2018;37:5253–73. doi:10.1007/s40314-018-0635-1.
20. Youssri YH, Hafez RM. Chebyshev collocation treatment of Volterra-Fredholm integral equation with error analysis. Arab J Math. 2020;9:471–80. doi:10.1007/s40065-019-0243-y.
21. Hafez RM, Youssri YH, Atta AG. Jacobi rational operational approach for time-fractional sub-diffusion equation on a semi-infinite domain. Contemp Math. 2023;4:853–476. doi:10.37256/cm.4420233594.
22. Hafez RM, Youssri YH. Spectral legendre-Chebyshev treatment of 2D linear and nonlinear mixed Volterra-Fredholm integral equation. Math Sci Lett. 2020;9:37–47.
23. Cebrián-Lacasa D, Parra-Rivas P, Ruiz-Reynés D, Gelens L. Six decades of the FitzHugh-Nagumo model: a guide through its spatio-temporal dynamics and influence across disciplines. J Phys Rep. 2024;1096:1–39. doi:10.1016/j.physrep.2024.09.014.
24. Dauby PC, Desaive TH, Croisier H, Kolh PH. Standing waves in the FitzHugh-Nagumo model of cardiac electrical activity. Phys Rev E Stat Nonlin Soft Matter Phys. 2006;73:021908. doi:10.1103/PhysRevE.73.021908.
25. Biasi N, Tognetti A. A computationally efficient dynamic model of human epicardial tissue. PLoS One. 2021;16:e0259066. doi:10.1371/journal.pone.0259066.
26. Werneck YB, dos Santos RW, Rocha BM, Oliveira RS. Replacing the FitzHugh-Nagumo electrophysiology model by physics-informed neural networks. In: Mikyška J, de Mulatier C, Paszynski M, Krzhizhanovskaya VV, Dongarra JJ, Sloot PM, editors. Computational science—ICCS 2023. Lecture notes in computer science. Vol. 14074, 2023.
27. Rufai MA, Kosti AA, Anastassi ZA, Carpentieri B. A new two-step hybrid block method for the FitzHugh-Nagumo model equation. Mathematics. 2024;12(1):51. doi:10.3390/math12010051.

28. Murray JD. Mathematical biology: I. An introduction. 3rd ed. Berlin, Germany: Springer; 2002.
29. Hinch EJ. Perturbation methods. Cambridge, UK: Cambridge University Press; 1991.
30. Ascher UM, Petzold LR. Computer methods for ordinary differential equations and differential-algebraic equations. Philadelphia, PA, USA: SIAM; 1998.
31. Stoer J, Bulirsch R. Introduction to numerical analysis. 3rd ed. Berlin, Germany: Springer; 2002.
32. Fletcher CAJ. Computational Galerkin methods. Berlin, Germany: Springer; 1984.
33. Szegõ G. Orthogonal polynomials. 4th ed. Providence, RI, USA: American Mathematical Society; 1975.
34. Canuto C, Hussaini MY, Quarteroni A, Zang TA. Spectral methods: fundamentals in single domains. Berlin, Germany: Springer; 2006.
35. Shen J, Tang T, Wang L. Spectral methods: algorithms, analysis and applications. Berlin, Germany: Springer; 2011.
36. Quarteroni A, Valli A. Numerical approximation of partial differential equations. Berlin, Germany: Springer; 1994.
37. Fornberg B. A practical guide to pseudospectral methods. Cambridge, UK: Cambridge University Press; 1998.
38. Peyret R. Spectral methods for incompressible viscous flow. Berlin, Germany: Springer; 2002.
39. Gottlieb D, Orszag SA. Numerical analysis of spectral methods: theory and applications. Philadelphia, PA, USA: Society for Industrial and Applied Mathematics; 1977.
40. Boyd JP. Chebyshev and fourier spectral methods. 2nd ed. Berlin, Germany: Springer; 2001.
41. Langtangen HP. Computational partial differential equations: numerical methods and diffpack programming. Berlin, Germany: Springer; 2003.
42. Hairer E, Nørsett SP, Wanner G. Solving ordinary differential equations i: nonstiff problems. 2nd ed. Berlin, Germany: Springer; 1993.
43. Press WH, Teukolsky SA, Vetterling WT, Flannery BP. Numerical recipes: the art of scientific computing. 3rd ed. Cambridge, UK: Cambridge University Press; 2007.
44. Iserles A. A first course in the numerical analysis of differential equations. 2nd ed. Cambridge, UK: Cambridge University Press; 2008.
45. Watson GN. A note on generalized hypergeometric series. P Lond Math Soc. 1925;23:13–5.
46. Abo-Gabal H, Zaky MA, Hafez RM, Doha EH. On Romanovski-Jacobi polynomials and their related approximation results. Numer Methods Partial Differ Equ. 2020;36(6):1982–2017. doi:10.1002/num.22513.
47. Rivlin TJ. An introduction to the approximation of functions. Courier Corporation; 1981.
48. Abdelkawy MA, Mohammad I, Waleed A. Robust and accurate numerical framework for multi-dimensional fractional-order telegraph equations using Jacobi/Jacobi-Romanovski spectral technique. Bound. Value Probl. 2024;2024:131. doi:10.1186/s13661-024-01944-1.
49. Abd-Elhameed WM, Al-Harbi MS, Atta AG. New convolved Fibonacci collocation procedure for the Fitzhugh-Nagumo non-linear equation. Nonlinear Eng. 2024;13:20220332. doi:10.1515/nleng-2022-0332.